
DNN’s Sharpest Directions Along the SGD Trajectory

Stanislaw Jastrzebski^{1,2}, Zachary Kenton², Nicolas Ballas³, Asja Fischer⁴,
 Yoshua Bengio⁵, Amos Storkey⁶

Abstract

Recent work has identified that using a high learning rate or a small batch size for Stochastic Gradient Descent (SGD) based training of deep neural networks encourages finding flatter minima of the training loss towards the end of training. Moreover, measures of the flatness of minima have been shown to correlate with good generalization performance. Extending this previous work, we investigate the loss curvature through the Hessian eigenvalue spectrum in the *early* phase of training and find an analogous bias: even at the beginning of training, a high learning rate or small batch size influences SGD to visit flatter loss regions. In addition, the evolution of the largest eigenvalues appears to always follow a similar pattern, with a fast increase in the early phase, and a decrease or stabilization thereafter, where the peak value is determined by the learning rate and batch size. Finally, we find that by altering the learning rate just in the direction of the eigenvectors associated with the largest eigenvalues, SGD can be steered towards regions which are an order of magnitude sharper but correspond to models with similar generalization, which suggests the curvature of the endpoint found by SGD is not predictive of its generalization properties.

1 Introduction

Deep Neural Networks (DNNs) are often massively over-parameterized [Zhang et al., 2016], yet show state-of-the-art generalization performance on a wide variety of tasks when trained with Stochastic Gradient Descent (SGD). While understanding the generalization capability of DNNs remains an open challenge, it has been hypothesized that SGD acts as an implicit regularizer, limiting the complexity of the found solution [Poggio et al., 2017, Advani and Saxe, 2017, Wilson et al., 2017, Jastrzebski et al., 2017].

Various links between the curvature of the final minima reached by SGD and generalization have been studied [Murata et al., 1994, Neyshabur et al., 2017]. In particular, it is a widely-held view that models corresponding to wide minima of the loss in the parameter space generalize better than sharp ones [Hochreiter and Schmidhuber, 1997, Shirish Keskar et al., 2016, Jastrzebski et al., 2017]. The existence of this empirical correlation between width of the final minima and generalization motivates our study.

Our work aims at enriching our understanding of the loss surface of DNNs and its interplay with SGD. We analyze the curvature along the SGD path in the early phase of training. We observe that the evolution of the largest eigenvalues follows a similar pattern for the different networks and datasets that we explore. Initially, SGD is in a region of broad curvature, and as the loss decreases, SGD visits

¹Jagiellonian University, staszek.jastrzebski@gmail.com

²MILA, Université de Montréal

³Facebook AI Research

⁴Ruhr-University Bochum

⁵CIFAR Senior Fellow

⁶School of Informatics, University of Edinburgh.

increasingly sharp regions, reaching a peak value influenced by the learning rate and batch size. At the end of this process, the loss surface along the sharpest direction resembles a bowl, with the property that an SGD step is typically too large to reach the floor (minimum) in this subspace. Afterwards, we observe a decrease or stabilization of the largest eigenvalues. See Fig. 1 for an illustration.

By proposing a variant of SGD which is steered towards sharp minima, whilst maintaining good generalization performance of the final model, we extend the work of Dinh et al. [2017] by providing empirical evidence that the relationship between the sharpness of minima and generalization might not be causal. Additionally, we observe that steering towards a sharp minima resulted in a slightly improved training speed.

2 Experimental setup and notation

We perform experiments mainly on Resnet-32⁷ and a simple convolutional neural network, which we refer to as SimpleCNN (details in Supplement F), and the CIFAR-10 dataset [Krizhevsky et al.]. SimpleCNN is a 4 layer CNN, achieving roughly 86% test accuracy on the CIFAR-10 dataset. Both of the models use standard data augmentation for CIFAR-10, Resnet-32 uses L2 regularization with a regularization parameter of 0.005. We additionally investigate the training of VGG-11 [Simonyan and Zisserman, 2014] on the CIFAR-10 dataset (we adapted the final classification layers for 10 classes) and of a bidirectional Long Short Term Memory (LSTM) model (following the “small” architecture employed by Zaremba et al. [2014], with dropout regularization) on the Penn Tree Bank (PTB) dataset.

Computing the full spectrum of the Hessian of the loss for reasonably large models is computationally infeasible. Therefore, we approximate the top K (less than 30) eigenvalues (ordered according to their absolute values) using the Lanczos algorithm [Lanczos, 1950, Dauphin et al., 2014], an extension of the power method, on approximately 5% of the training data. Where applicable, the eigenvalues are estimated without applying any regularization apart from L2 (such as dropout, batch normalization or data augmentation). All models are trained using SGD⁸. Our main focus is on SGD using a constant learning rate and batch size.

In the following we will fix the notation. We will use t to refer to epoch or iteration, depending on the context. By η and S we denote the SGD learning rate and batch size, respectively. \mathbf{H} is the Hessian of the empirical loss at the current parameters evaluated on the training set. $\rho(\mathbf{H})$ is the maximum eigenvalue, which is equivalent to the spectral norm of \mathbf{H} . The top K normalized eigenvectors of \mathbf{H} are denoted by \mathbf{e}_i , for $i \in \{1, \dots, K\}$. We will refer to the mini-batch gradient calculated based on a batch of size S as $\mathbf{g}^{(S)}(t)$. We will often consider the projection of this gradient onto one of the top eigenvectors, given by $\tilde{\mathbf{g}}_i(t) = \tilde{g}_i(t)\mathbf{e}_i(t)$, where $\tilde{g}_i(t) \equiv \langle \mathbf{g}^{(S)}(t), \mathbf{e}_i(t) \rangle$. We will approximate the expected norm of the stochastic step-size along an eigenvector $\eta \mathbb{E}(|\tilde{\mathbf{g}}_i(t)|)$ with the average norm of an SGD step $\overline{\Delta\theta(t)}_i$ over ten examples of mini-batch gradients using batch-size S .

3 SGD is biased towards a flat region early on in training

In this section we investigate how the curvature of the loss function along the path found by SGD evolves during training. We highlight that SGD, with large learning rate or a small batch size, is biased towards flat regions of the loss surface already in the early phase of training.

3.1 Loss curvature along the SGD path

We first investigate how the curvature in the sharpest directions evolves during training for both SimpleCNN and Resnet-32 models. As shown in Fig. 2 (top) the spectral norm (which corresponds to the largest eigenvalue), as well as the other tracked eigenvalues, grows in the first epoch up to a maximum value. After reaching this maximum value, we observe a relatively steady decrease of the largest eigenvalues for the SimpleCNN model, and a stabilization for the Resnet-32 model. Further investigation reveals that the difference stems from the use of L2 regularization in the case of

⁷We removed Batch Normalization layers, and used an initialization scaled by depth of the network suggested by [Taki, 2017].

⁸We found that results generalize to SGD with momentum, additional results are reported in the Supplement.

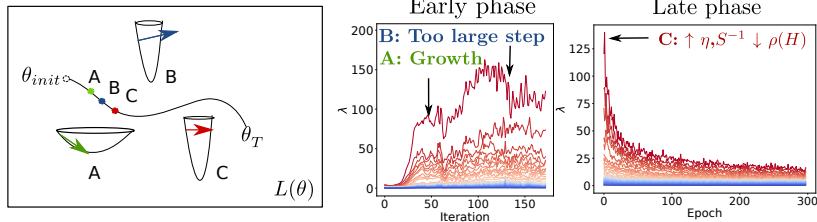


Figure 1: Outline of the phenomena discussed in the paper. **Left:** Schematic illustration of the evolution of the loss surface along the sharpest direction during training. Curvature along this direction initially grows (A). In most iterations, we find the loss surface along the sharpest direction to resemble a bowl, such that SGD crosses its *minima*, often taking a *too large step* (B and C). Finally, curvature stabilizes or decays with a peak value determined by learning rate and batch size (C, see also right). **Right two:** Representative example of the evolution of the top 30 (decreasing, red to blue) eigenvalues of the Hessian for a SimpleCNN model during training (with $\eta = 0.005$).

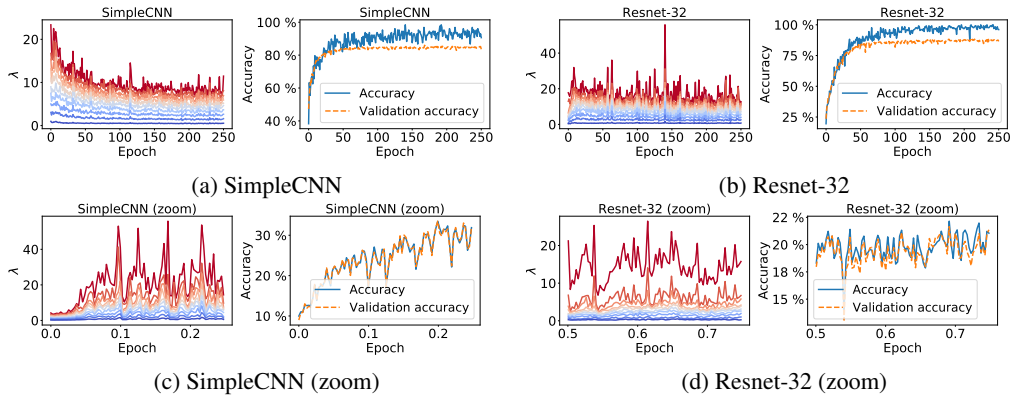


Figure 2: **Top:** Evolution of the top 10 eigenvalues of the Hessian for SimpleCNN and Resnet-32 trained on the CIFAR-10 dataset with $\eta = 0.1$ and $S = 128$. **Bottom:** Zoom on the evolution of the top 10 eigenvalues in the selected range of iterations in the beginning of training. Oscillatory-like evolution and a sharp growth of the largest eigenvalues are visible. Training and test accuracy of the corresponding models are provided for reference. Resnet-32 and SimpleCNN achieve 88% and 86% test accuracy, respectively.

Resnet-32, see Fig. 7 in the Supplement⁹. We also note that for low learning rates or large batch sizes the phase in which the spectral norm grows can take many epochs, as shown in Fig. 3.

To closer investigate the evolution of the curvature in the first epochs, we track the eigenvalues in each iteration in the beginning of training, see Fig. 2 (bottom). We observe that initially the largest eigenvalues grow rapidly. After reaching some maximum value, the largest eigenvalues follow an stochastic oscillatory-like behaviour, which is present also in the evolution of the accuracy.

Next, we investigate how the choice of learning rate and batch size impacts the SGD path in terms of its curvatures. Fig. 3 shows the evolution of the two largest eigenvalues of the Hessian during training of the SimpleCNN on CIFAR-10 for different values of η and S . We observe in this figure that a larger learning rate or a smaller batch-size correlates with a smaller and earlier peak of the spectral norm and the subsequent largest eigenvalue. Additionally we found that momentum has an analogous effect – using a larger momentum led to a smaller peak of spectral norm, see Fig. 16 in the Supplement.

These results show that the learning rate and batch size not only influence the SGD endpoint maximum curvature (as characterized by Jastrzebski et al. [2017]), but also impact the whole SGD trajectory. A high learning rate or small batch size limits the maximum spectral norm along the path found by SGD from the beginning of training. We stress that due to our focus on the early phase of training we

⁹We observed in some runs a sharp drop in $\rho(\mathbf{H})$ in the first iterations, which seemed to be related to large scaled initializations.

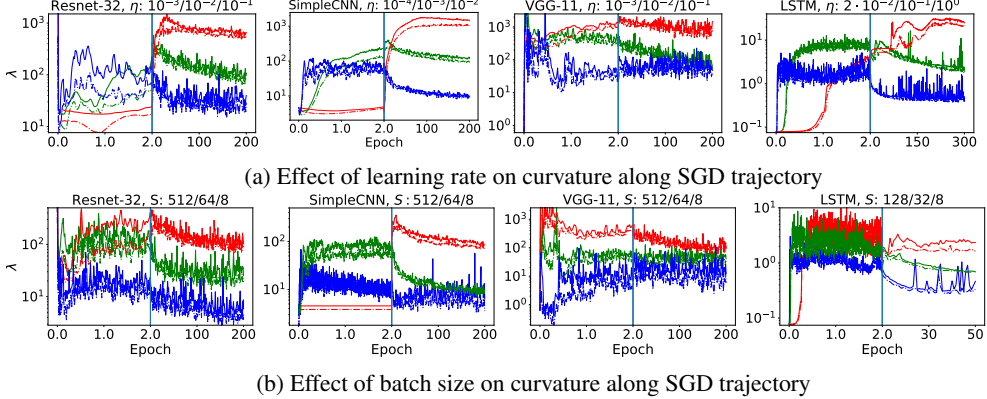


Figure 3: Evolution of the two largest eigenvalues of the Hessian for Resnet-32, SimpleCNN, VGG11 and LSTM (trained on the PTB dataset) models on a log-scale for different learning rates (top) and batch-sizes (bottom). Red/green/blue correspond to increasing η and decreasing S in each figure. Left side of the vertical blue bar in each plot corresponds to the first two epochs of training. Larger learning rate or a smaller batch-size correlates with a smaller and earlier peak of the spectral norm and the subsequent largest eigenvalue. Peak position gets later from blue to green to red, indicating that the sharpest region is reached earlier for higher learning rate and lower batch size.

discussed SGD with a constant learning rate and batch size. We report some additional results using learning rate schedules in Fig. 15 in the Supplement.

3.2 Loss surface shape along the sharpest direction

The largest eigenvalues of the Hessian describe the loss surface curvature at a precise point locally, however it is not clear what the overall shape of the local loss surface looks like on a bigger scale. In this section, we investigate how the shape of the loss evolves in the direction of the eigenvector corresponding to the largest eigenvalue.

Fig 4 (left) shows how the loss changes along its sharpest direction in the first few epochs of training. Specifically, we evaluate $L(\theta(t) + k\bar{\Delta\theta}_1(t))$, where $\theta(t)$ is the current parameter vector, $\bar{\Delta\theta}_1(t)$ is the approximated expected norm of the SGD step along the top eigenvector, i.e. of $\eta\mathbb{E}(|\tilde{g}_1(t)|)$, and k is an interpolation parameter (we use $k \in [-8, 8]$). One can interpret $\bar{\Delta\theta}_1(t)$ as the typical step-size along the top eigenvector.

For both SimpleCNN and Resnet-32 models, we observe that the loss starts to show a bowl-like structure in the largest eigenvalue direction after four epochs. In addition, we observe that the current parameter estimate found by SGD appears to be close to the floor (minimum) of the loss surface along the sharpest direction early on for the considered step size. We also observe that the bowl-like structure around the current parameter estimate appears to be relatively “narrow” compared to the average SGD step-size. To quantify this relation between $\bar{\Delta\theta}_1(t)$ and the curvature we report the smallest k , k_{min} , such that $L(\theta(t) + k\bar{\Delta\theta}_1(t))$ changes at least by 1%/10% compared to $L(\theta(t))$. We average k_{min} over the last 100 iterations. For SimpleCNN and Resnet-32 the average k_{min} that lead to a change of 1% (10%) was 3.36 (5.52) and 1.56 (4.08), respectively.

To further investigate how the loss changes along the sharpest direction we look at how the loss value changes on average when moving from the current parameter estimate of SGD by taking a step only along the sharpest direction - see Fig. 4 right. For all training iterations, we compute $\mathbb{E}[L(\theta(t) - \alpha\eta\tilde{g}_1(t))] - L(\theta(t))$, for $\alpha \in \{0.25, 0.5, 1, 2, 4\}$, and keep the same learning rate η used during training. The expectation is approximated by an average over 10 different mini-batch gradients of size $S = 128$. We find that $\mathbb{E}[L(\theta(t) - \alpha\eta\tilde{g}_1(t))] - L(\theta(t))$ increases relative to $L(\theta(t))$ for $\alpha > 1$, and decreases for $\alpha < 1$. For SimpleCNN we find that $\alpha = 2$ and $\alpha = 4$ lead to a 2.1% and 11.1% increase in loss, while $\alpha = 0.25$ and $\alpha = 0.5$ both lead to a decrease of approximately 2%. For Resnet-32 we observe a 3% and 13.1% increase for $\alpha = 2$ and $\alpha = 4$, and approximately a 3% decrease for $\alpha = 0.25$ and $\alpha = 0.5$, respectively. Additionally, we see that there starts to be a large increase in loss for steps with $\alpha = 1$ and $\alpha = 2$, approximately at the same time at which the bowls

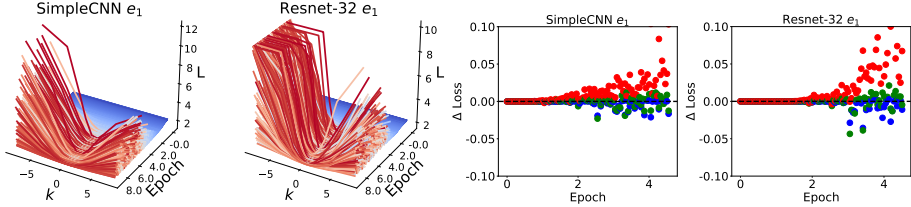


Figure 4: **Left two:** Loss surface along the top eigenvector at the beginning of training of SimpleCNN and ResNet-32 on CIFAR-10. At iteration t we plot the loss $L(\theta(t) + k\bar{\Delta\theta}_1(t))$, around the current parameters $\theta(t)$, where $\bar{\Delta\theta}_1(t)$ is the expected norm of the SGD step along the top eigenvector. The x -axis represents the interpolation parameter k , the y -axis the epoch, and the z -axis the loss value. The color of each line indicates the corresponding spectral norm (increasing from blue to red). SimpleCNN (ResNet-32) is trained with $\eta = 0.005$, $S = 128$ (with $\eta = 0.025$, $S = 128$), learning curves are provided in the Supplement. After a couple of epochs the loss in the subspace starts to have a bowl-like shape and SGD appears to be close to its minimum in the sharpest direction. **Right two:** Average change in loss $\mathbb{E}[L(\theta(t) - \alpha\eta\tilde{g}_1(t))] - L(\theta(t))$, for $\alpha = 0.5, 1, 2$ corresponding to red, green, and blue, respectively. On average, the SGD step-size in the direction on the sharpest direction does not minimize the loss, however, reducing the step size by half can further minimize the loss in this sharpest direction. The red points further show that increasing the step-size by two consistently increases the loss, on average.

appear in the plots in the left of Fig. 4. These results suggest that SGD, with a constant learning rate, quickly settles to a region where the typical step-size of SGD is “too large” with respect to the curvature in the top eigenvector direction and this prevents it from reaching the floor (minimum) of the bowl-like structure in this specific direction. We note that a related bouncing behavior of SGD has concurrently been observed by Xing et al. [2018].

We report training and validation accuracy and additional results in Supplement B. We observe a similar phenomena happening along the 3rd eigenvector. Also, similar results hold for different η , and when training with Batch Normalization.

3.3 How SGD steers to and away from sharp regions in the early phase

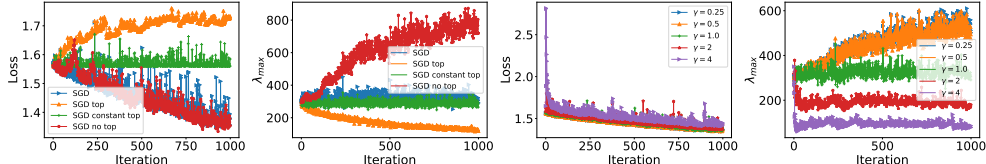


Figure 5: Evolution of the loss and the top eigenvalue during training with variations of SGD with parameter updates restricted to certain subspaces. All variants are initialized at the last iteration in Fig. 1. **Left two:** SGD variant with parameter updates restricted to certain subspaces. An SGD variant (orange) that follows at each iteration only the projection of the gradient on the top eigenvector of \mathbf{H} effectively finds a region with lower $\rho(\mathbf{H})$ but increases the loss, while a variant subtracting this projection from the gradient (red), finds a sharper region while achieving a similar loss level as vanilla SGD (blue). **Right two:** SGD variant using a rescaled by factor γ learning rate along the top eigenvector. Variants using $\gamma > 1$ are able to find wider regions, while variants using $\gamma < 1$ move to a sharper region.

The results of the previous sections show that SGD follows a path along which the sharpness *grows* in the early phase. In this section we are interested in the dynamics behind this initial growth and its stop. We will contrast SGD dynamics along the sharpest with dynamics along flatter directions of the Hessian at the iteration at which the loss surface along the sharpest direction starts to resemble a bowl, as described in the previous section.

We investigated the behavior of SGD variants with parameter updates restricted to certain subspaces. Results are shown in the left two plots of Fig. 5. We trained the same SimpleCNN model as used in

the experiments depicted in Fig. 1. For each experiment the model was initialized with the parameters reached by SGD in the previous experiment at the end of epoch 4 (when the spectral norm has already stabilized, as visible in Fig. 1). The parameter updates used by the three SGD variants, which are compared to vanilla SGD (blue), are based on the mini-batch gradient $\mathbf{g}^{(S)}$ as follows: **variant 1** (SGD top, orange) only updates the parameters based on the projection of the gradient on the top eigenvector direction, i.e. $\mathbf{g}(t) = \langle \mathbf{g}^{(S)}(t), \mathbf{e}_1(t) \rangle \mathbf{e}_1(t)$; **variant 2** (SGD constant top, green) performs updates along the constant direction of the top eigenvector $\mathbf{e}_1(0)$ of the Hessian in the first iteration, i.e. $\mathbf{g}(t) = \langle \mathbf{g}^{(S)}(t), \mathbf{e}_1(0) \rangle \mathbf{e}_1(0)$; **variant 3** (SGD no top, red) removes the gradient information in the direction of the top eigenvector, i.e. $\mathbf{g}(t) = \mathbf{g}^{(S)}(t) - \langle \mathbf{g}^{(S)}(t), \mathbf{e}_1(t) \rangle \mathbf{e}_1(t)$.

As the experimental results of variant 1 demonstrate, taking gradient paths only along the top eigenvalue direction increases the loss, whilst decreasing the spectral norm. This means this SGD variant is finding wider regions compared to standard SGD but is not decreasing the loss. The updates in the fixed direction (corresponding to the top eigenvector in the first epoch) made by variant 2 (green) neither affect loss nor spectral norm, even in the beginning - this implies that during training the top eigenvectors must be changing their direction fast enough to induce a movement out of the subspace spanned by the initial top eigenvector. From the results for variant 3 (red) we see that if we remove the top eigenvector gradient projection from the gradient, the loss is reduced in a similar manner as by vanilla SGD but the spectral norm continues to increase, implying that the movement in the top eigenvector direction plays an important role in stopping the growth of the spectral norm.

In the previous experiment each SGD variant followed only a subset of eigenvectors of the Hessian. To investigate if the results are affected by considering SGD restricted to these subspaces, in a second experiment we investigate the behavior of SGD when it follows all directions in the parameter space but with rescaled learning rates. Specifically, we consider a SGD variant, again restarted at the last iteration from Fig. 4, using a re-scaled learning rate $\eta' = \gamma\eta$ along \mathbf{e}_1 . In accordance, to the results of the previous experiment we find, as shown in Fig. 5, that this SGD variant with $\gamma < 1$ (orange and blue in the figure) moved to regions corresponding to larger $\rho(\mathbf{H})$. Conversely, variants corresponding to $\gamma > 1$ (red and purple in the figure) moved to regions corresponding to lower $\rho(\mathbf{H})$ very quickly. All variants were able to overall reduce loss.

The take-home message from this subsection is that SGD updates in the top eigenvector direction strongly influence the overall path taken in the early phase of training, influencing both the evolution of the loss value as well as the sharpness of the corresponding loss curvature; if we only follow the top eigenvector, we get to wider regions but don't reach lower loss values, and conversely, if we ignore this top eigenvector we reach lower loss values but sharper regions.

4 Finding sharp minima maintaining generalization

The discussed dynamics in the early phase of training suggest a straightforward way to steer SGD towards a sharp or wide minima: by using a smaller or larger learning rate η along the sharpest directions, and hence decreasing or increasing the length of an SGD step in these directions. [Dinh et al. \[2017\]](#) argued theoretically there is no causal link between the width of the regions and generalization by showing the existence of sharp regions that generalize well. Following this line of inquiry, we empirically investigate SGD variants that can be steered towards wider or sharper regions. In contrast to [Dinh et al. \[2017\]](#) the sharp regions that we investigate here are the endpoints of an optimization procedure, rather than a result of a reparametrization, which may or may not be reachable using gradient based optimization.

We refer to our variant of SGD as Nudged SGD (NSGD), which we already investigated in the previous section. Instead of using the standard SGD update, $\Delta\theta(t) = -\eta\mathbf{g}^{(S)}(t)$, NSGD uses a different learning rate, $\eta' = \gamma\eta$, along just the top K eigenvectors, while following the normal SGD gradient along all the others directions (note that, for instance, Resnet-32 has $\approx 3 * 10^5$ parameters). We compare the sharpness of the reached endpoint by both computing the Frobenius norm (approximated based on the top 5 eigenvectors) and the spectral norm of the Hessian.

We ran experiments with Resnet-32 and SimpleCNN on CIFAR-10¹⁰. We investigated NSGD with differently rescaled learning rates, i.e. with $\gamma \in \{0.01, 0.1, 1, 10\}$. We recomputed the top

¹⁰We increased the number of filters to 100 (from 64) and the size of kernels to 5 (from 3), which sped up optimization.

γ	$\ \mathbf{H}\ _F$	Test acc.	Val. acc. (50)	Loss	Dist.	$\rho(W)$
0.01	483/1, 559	87.4%	58.3%	0.06067	22.99	159.81
0.1	350/816	87.2%	57.0%	0.06128	23.41	161.42
1.0	103/121	86.6%	54.0%	0.06443	24.62	166.47
10	54/19	85.2%	43.8%	0.10194	29.39	187.77
SGD(0.1)	9/13	89.7%	82.6%	0.10787	34.90	216.35
SGD(0.005)	278/511	85.6%	41.7%	0.08392	21.21	147.17
SGD(0.0025)	683/1, 190	84.8%	30.9%	0.10304	18.65	131.73
γ	$\ \mathbf{H}\ _F$	Test acc.	Val. acc. (50)	Loss	Dist.	$\rho(W)$
0.01	307/422	87.0%	82.8%	0.00761	20.50	60.06
0.1	126/248	87.2%	82.7%	0.00206	20.68	60.20
1.0	8/12	86.4%	81.5%	0.00252	20.95	60.38
10	54/1	85.3%	74.9%	0.00330	23.36	63.52
SGD(0.1)	1/0	87.9%	85.2%	0.00037	62.53	120.13
SGD(0.005)	45/35	86.0%	77.6%	0.00937	17.10	55.55
SGD(0.0025)	149/183	85.3%	71.8%	0.02454	14.37	52.39

Table 1: Nudged-SGD using a different rescaled learning rate ($\eta' = \gamma\eta$) along the 5 sharpest directions steers towards an order of magnitude sharper or wider minima, depending on γ , for Resnet-32 model (Top) and SimpleCNN (Bottom). *We find sharper minima with similar generalization performance.* Columns report: the Frobenius norm of the Hessian approximated at the best validation point, and its average value in the last 10 epochs; test accuracy at the best validation epoch; validation achieved after 50 epochs; average loss in the last 10 epochs; distance of the parameters from the initialization to the best validation epoch parameters; average spectral norm of weight matrices. Experiments were performed with $\eta = 0.01$ and $S = 128$. In the last rows we report SGD using $\eta \in \{0.0025, 0.005, 0.1\}$.

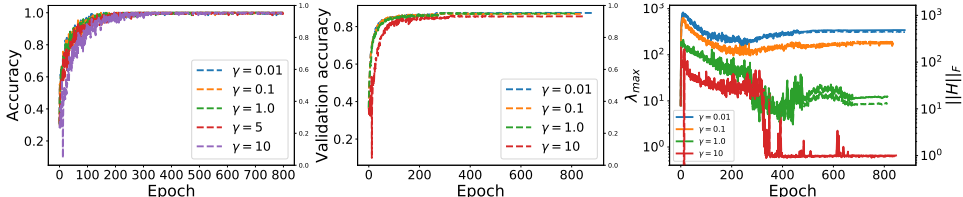


Figure 6: Nudged SGD (NSGD) using a different learning rate ($\eta' = \gamma\eta$) along the 5 sharpest directions. **Left two:** Training and validation accuracy of different NSGD runs. **Right:** Spectral norm (solid) and Frobenius norm (dashed, approximated using the top 5 eigenvalues), plotted on a log scale, of different SGDE runs. Experiment is run on SimpleCNN model and the CIFAR-10 dataset.

eigenvectors at the beginning of each epoch. To ensure existence of a generalization gap, a small learning rate $\eta = 0.01$ was used for both models¹¹. We rescaled the parameter update via a multiplication with gamma along the top $K = 5$ eigenvectors, which as we observed led to larger changes in sharpness than just rescaling in the direction of the first eigenvector. To ensure convergence, we automatically decay η by a factor of 10 when reaching a plateau of validation accuracy. Fig. 6 shows results for SimpleCNN on CIFAR-10, and Tab. 1 summarizes the results for all experiments on CIFAR-10.

By adapting γ , NSGD can be steered towards an order of magnitude sharper or wider minima. For $\gamma = 1.0$ (i.e. vanilla SG) the final minima Frobenius norm is 13 and 126 for SimpleCNN and Resnet-32, respectively (see Tab. 1, first column). In comparison $\gamma = 0.01$ leads to final Frobenius norm of 447 and 1,631, respectively; while $\gamma = 10$ resulted in a a norm of 1 and 20. The corresponding loss values are similar, as reported in Tab. 1. We note that NSGD is able to steer more effectively towards a sharper minima than a wider minima, likely due to the added instability induced by using a larger η .

¹¹NSGD was also more effective in finding wider or sharper minima for a lower η . We attribute it to the fact that we estimate eigenvectors only every epoch, which might be not frequent enough in the case of a large η , for which the eigenbasis of the Hessian might change rapidly.

along the top eigenvectors, as visible in Fig. 6 (red curve). Finally, we found a smaller γ to slightly reduce the overall distance traveled from the initialization, see Tab. 1 (fifth column). However, the overall changes in distance due to using different γ are small compared to changes induced by using a different η . Similar conclusions hold for the spectral norm of weights, see Tab. 1 (last column).

While NSGD using $\gamma < 1$ results in finding an order of magnitude sharper minima, we observe that the generalization performance of the corresponding model is not reduced. We select the epoch corresponding to the best validation accuracy. The baseline (SGD, corresponding to NSGD with $\gamma = 1.0$) reached 86.4% and 86.6% test accuracy, for Resnet-32 and SimpleCNN, respectively. In comparison, NSGD with $\gamma = 0.01$ found minima corresponding to 87.0% and 87.4% test accuracy, but an order of magnitude larger sharpness (measured either by the Frobenius norm or the spectral norm) compared to the baseline. On the contrary, finding a wider minima ($\gamma > 1$) correlated with worse generalization, perhaps due to the added instability. Additionally, we found that smaller γ to be correlated with faster optimization, as indicated by the validation accuracy reached after 50 epochs, see Tab. 1 (4th column).

To summarize, we have proposed a straightforward modification to SGD capable of finding either wider or sharper minima. Additionally, we observed some benefit of using a lower η along the sharpest directions, as in all experiments initial training speed was improved. For the most experiments, the validation performance was not affected by finding an order of magnitude sharper final minima. Additionally, finding a wider minima correlated with *worse* validation performance, which goes against commonly-held views on width and generalization. Similar conclusions hold for experiments on the CIFAR-100 dataset and for SGD using momentum, as shown in Supplement C.

5 Related work

Tracking the Hessian: The top eigenvalues of the Hessian of the loss of neural networks were investigated previously but most of these prior papers focused on the end of training, rather than the whole training trajectory. Some notable exceptions are: [LeCun et al. \[1998\]](#) who first track the Hessian spectral norm, and the initial growth is reported (though not commented on). [Sagun et al. \[2016\]](#) report that the spectral norm of the Hessian reduces towards the end of training. [Shirish Keskar et al. \[2016\]](#) observe that sharpness grows initially for large batch-size, but only decays for small batch-size. Our observations are much more detailed, and in particular, we observe the growth and decay for all batch sizes.

Wider minima generalize better: [Hochreiter and Schmidhuber \[1997\]](#) argued that wide minima should generalize well. [Shirish Keskar et al. \[2016\]](#) provided empirical evidence that the width of the endpoint minima found by SGD correlates with generalization, while the width is anti-correlated to the batch-size. [Jastrzebski et al. \[2017\]](#) extended this by finding a correlation of the width and the learning rate to batch-size ratio. [Dinh et al. \[2017\]](#) demonstrated the existence of reparametrizations of networks which keep the loss value and generalization performance constant while increasing sharpness of the associated minimum, implying it is not just the width of a minimum which determines the generalization.

Role of anisotropic noise in stochastic gradient descent. Our work is closely related to a recent study on the role of anisotropic noise for generalization in SGD by [Zhu et al. \[2018\]](#). In particular, they study the importance of noise along the top eigenvector for escaping at the *endpoint* by comparing SGD with other optimizer variants starting from the global minima found by gradient descent. In contrast we show that from the beginning of training SGD visits bowl-like structures in the subspace of the top eigenvectors and the escaping-like process happens already within the early phase of training. Concurrent with this work [Xing et al. \[2018\]](#) also study how SGD navigates the DNN loss landscape. In particular, by interpolating the loss between parameter values at consecutive iterations they show it is roughly-convex, whereas we show a related phenomena by investigating the loss in the subspace of eigenvectors of the top eigenvalues of the Hessian.

6 Conclusions

We found that for high learning rate, or small batch size, SGD finds a flat region of the loss surface, already early on in training. At the end of this process the loss surface along the directions of the top eigenvector resembles a bowl. Based on further analysis, we constructed a simple variant of

SGD, which can be steered towards sharper with similar generalization performance, while slightly improving training speed. In future work it should be investigated how the discussed phenomena extend to other models, datasets, and loss functions.

We hope this study will suggest new directions for exploring links between generalization and loss surface curvature, as well as help to improve our understanding of the interplay between SGD and the loss surface of DNNs.

Acknowledgements

SJ was in part supported by Grant No. DI 2014/016644 from Ministry of Science and Higher Education, Poland and No. 2017/25/B/ST6/01271 from National Science Center, Poland. Work at MILA was funded by NSERC, CIFAR, and Canada Research Chairs. This project has received funding from the European Union’s Horizon 2020 research and innovation programme under grant agreement No 732204 (Bonseyes). This work is supported by the Swiss State Secretariat for Education, Research and Innovation (SERI) under contract number 16.0159. The opinions expressed and arguments employed herein do not necessarily reflect the official views of these funding bodies.

References

Madhu S Advani and Andrew M Saxe. High-dimensional dynamics of generalization error in neural networks. *arXiv preprint arXiv:1710.03667*, 2017.

Yann Dauphin, Razvan Pascanu, Çaglar Gülcehre, Kyunghyun Cho, Surya Ganguli, and Yoshua Bengio. Identifying and attacking the saddle point problem in high-dimensional non-convex optimization. *CoRR*, abs/1406.2572, 2014. URL <http://arxiv.org/abs/1406.2572>.

Laurent Dinh, Razvan Pascanu, Samy Bengio, and Yoshua Bengio. Sharp minima can generalize for deep nets. *arXiv preprint arXiv:1703.04933*, 2017.

Sepp Hochreiter and Jürgen Schmidhuber. Flat minima. *Neural Computation*, 9(1):1–42, 1997.

Stanisław Jastrzebski, Zachary Kenton, Devansh Arpit, Nicolas Ballas, Asja Fischer, Yoshua Bengio, and Amos Storkey. Three factors influencing minima in sgd. *arXiv preprint arXiv:1711.04623*, 2017.

Alex Krizhevsky, Vinod Nair, and Geoffrey Hinton. Cifar-10 (canadian institute for advanced research). URL <http://www.cs.toronto.edu/~kriz/cifar.html>.

Cornelius Lanczos. An iteration method for the solution of the eigenvalue problem of linear differential and integral operators. *J. Res. Natl. Bur. Stand. B*, 45:255–282, 1950. doi: 10.6028/jres.045.026.

Yann LeCun, Léon Bottou, Genevieve B. Orr, and Klaus-Robert Müller. Efficient backprop. In *Neural Networks: Tricks of the Trade, This Book is an Outgrowth of a 1996 NIPS Workshop*, pages 9–50, London, UK, UK, 1998. Springer-Verlag. ISBN 3-540-65311-2. URL <http://dl.acm.org/citation.cfm?id=645754.668382>.

Noboru Murata, Shuji Yoshizawa, and Shun ichi Amari. Network information criterion-determining the number of hidden units for an artificial neural network model. *IEEE transactions on neural networks*, 5:865–72, 1994.

Behnam Neyshabur, Srinadh Bhojanapalli, David McAllester, and Nathan Srebro. Exploring generalization in deep learning. *CoRR*, abs/1706.08947, 2017. URL <http://arxiv.org/abs/1706.08947>.

Tomaso Poggio, Kenji Kawaguchi, Qianli Liao, Brando Miranda, Lorenzo Rosasco, Xavier Boix, Jack Hidary, and Hrushikesh Mhaskar. Theory of deep learning iii: explaining the non-overfitting puzzle. *arXiv preprint arXiv:1801.00173*, 2017.

Levent Sagun, Léon Bottou, and Yann LeCun. Singularity of the hessian in deep learning. *arXiv preprint arXiv:1611.07476*, 2016.

N. Shirish Keskar, D. Mudigere, J. Nocedal, M. Smelyanskiy, and P. T. P. Tang. On Large-Batch Training for Deep Learning: Generalization Gap and Sharp Minima. *ArXiv e-prints*, September 2016.

Karen Simonyan and Andrew Zisserman. Very deep convolutional networks for large-scale image recognition. *CoRR*, abs/1409.1556, 2014. URL <http://arxiv.org/abs/1409.1556>.

Masato Taki. Deep residual networks and weight initialization. *CoRR*, abs/1709.02956, 2017. URL <http://arxiv.org/abs/1709.02956>.

Ashia C Wilson, Rebecca Roelofs, Mitchell Stern, Nathan Srebro, and Benjamin Recht. The marginal value of adaptive gradient methods in machine learning. 2017.

C. Xing, D. Arpit, C. Tsirigotis, and Y. Bengio. A Walk with SGD. *ArXiv e-prints*, February 2018.

Wojciech Zaremba, Ilya Sutskever, and Oriol Vinyals. Recurrent neural network regularization, 2014. URL <https://arxiv.org/abs/1409.2329>.

Chiyuan Zhang, Samy Bengio, Moritz Hardt, Benjamin Recht, and Oriol Vinyals. Understanding deep learning requires rethinking generalization. *arXiv preprint arXiv:1611.03530*, 2016.

Z. Zhu, J. Wu, B. Yu, L. Wu, and J. Ma. The Regularization Effects of Anisotropic Noise in Stochastic Gradient Descent. *ArXiv e-prints*, February 2018.

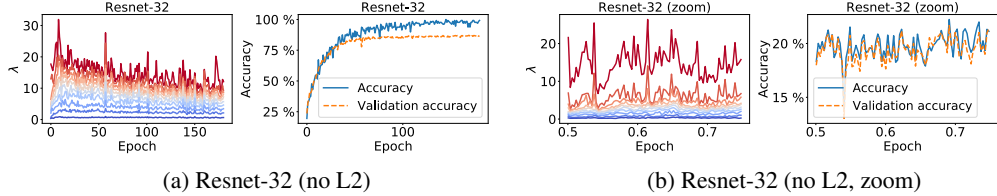


Figure 7: **Left:** Evolution of the top 10 eigenvalues of the Hessian for Resnet-32 trained on the CIFAR-10 dataset with $\eta = 0.1$ and $S = 128$, without L2 regularization. **Right:** Zoom on the evolution of the top 10 eigenvalues in the selected range of iterations in the beginning of training.

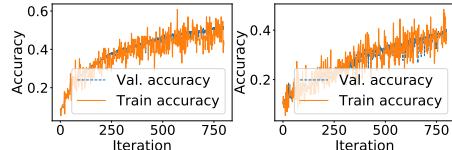


Figure 8: Training and validation accuracy for experiments in Fig 4. Left corresponds to SimpleCNN. Right corresponds to Resnet-32.

A Additional results for Sec. 3.1

In Sec. 3.1 we observed a difference between evolution of the largest eigenvalues of the Hessian between SimpleCNN and Resnet-32 model. Resnet-32 was trained using L2 regularization. To investigate this, in Fig. 7 we report evolution of the largest eigenvalues of the Hessian of Resent-32 model trained without L2 regularization. We observe a consistent decay of the largest eigenvalues, as for SimpleCNN, which suggests that the difference was due to the use of L2 regularization.

B Additional results for Sec. 3.2

In Fig. 8 we report the corresponding training and validation curves for the experiments depicted in Fig. 4. Next, we plot an analogous visualization as in Fig. 4, but for the 3rd and 5th eigenvector, see Fig. 9 and Fig. 10, respectively.

To ensure that the results do not depend on the learning rate, we rerun the Resnet-32 and SimpleCNN experiments with $\eta = 0.01$, see Fig. 11. We also examine the effect of batch normalization on Resnet-32 in Fig. 12.

C Additional results for Sec. 4

Here we report additional results for Sec. 4. First, we rerun the same experiment as reported in Tab. 1 and Fig. 6, but with momentum 0.9. We find that the general conclusions are the same: NSGD can be effectively steered towards a sharp minima or wide minima by just adjusting the γ parameter, and importantly is able to find a well generalizing sharp minimum. Results are reported in Tab. 3, Fig. 13 (SimpleCNN model) and Fig. 14 (Resnet32 model).

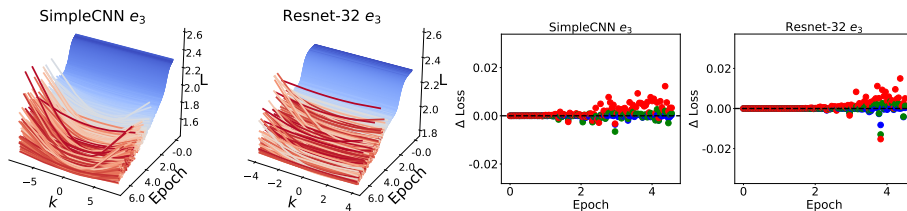


Figure 9: Similar to Fig 4 but for the third eigenvector. We see that the loss surface is flatter (note different scale on z axis) in this direction and less likely to overshoot within a few gradients steps.

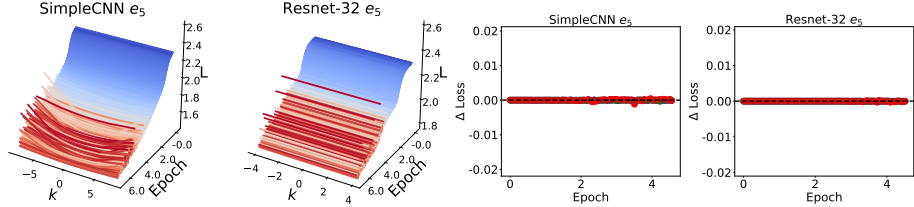


Figure 10: Similar to Fig 4 but for the fifth eigenvector. We see that the loss surface is much flatter in this direction (note different scale on z axis) and less likely to overshoot within a few gradients steps.

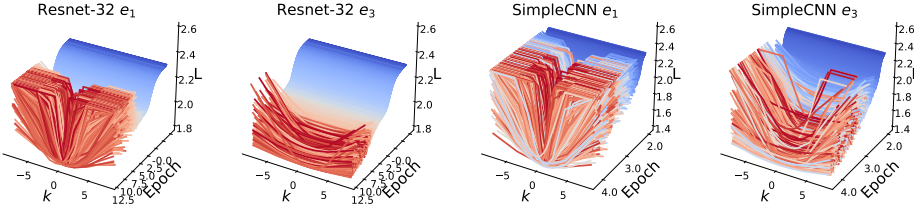


Figure 11: Similar to Fig 4 but for Resnet-32 (top) and SimpleCNN (bottom) with $\eta = 0.01$. Note different scale on z axis. **Left column:** 1st eigenvector. **Right column:** 3rd eigenvector.

Finally, we rerun the experiment on CIFAR100 dataset. Results are reported in Tab. 2. Again, similar conclusions hold as in the experiments on the CIFAR-10 dataset.

D Impact of learning rate schedule

In the paper we focused mostly on SGD using constant η and S . We report here the evolution of $\rho(\mathbf{H})$ for VGG-11 on the CIFAR-10 dataset for a step-wise and a cyclic learning rate schedule. We observe that, in these experiments, $\rho(\mathbf{H})$ seems to decay after the decrease of learning rate. This is in accordance with the general decay of the largest eigenvalues after achieving the peak value. See Fig. 15 for details. However, we observed in other experiments, omitted here for clarity, that after the decrease of learning rate the spectral norm can start to grow again. We leave the investigation of this phenomena for future work.

E Impact of using momentum

In the paper we focused mostly on experiments using plain SGD, without momentum. In this section we report that large momentum similarly to large η leads to a reduction of spectral norm of the Hessian, see Fig. 16 for results on the VGG11 network on CIFAR10 and CIFAR100.

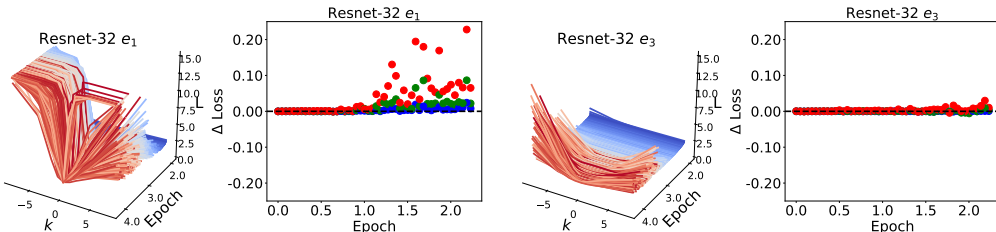


Figure 12: Similar to Fig 4 but for Resnet-32 with Batch Normalization ($\eta = 0.0025$, $S = 128$). **Top:** is first eigenvector. **Bottom:** third eigenvector.

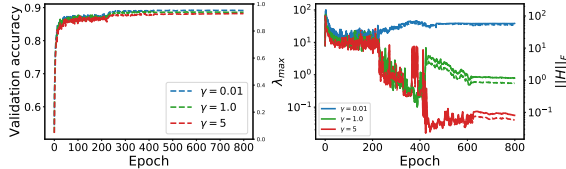


Figure 13: Same experiment as in Fig. 6, but run using momentum (0.9).

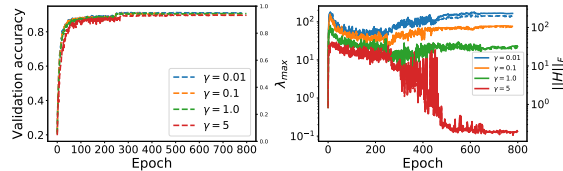


Figure 14: Same experiment as in Fig. 6, but run using Resnet32 and momentum (0.9).

γ	$ \mathbf{H} _F$	Test acc.	Val. acc. (50)	Loss	Dist.	$\rho(W)$
0.01	704/1,179	56.5%	14.1%	0.43895	30.68	185.19
0.1	590/869	55.7%	13.9%	0.51539	29.15	175.84
1.0	219/326	53.1%	12.7%	0.53788	31.54	185.99

γ	$ \mathbf{H} _F$	Test acc.	Val. acc. (50)	Loss	Dist.	$\rho(W)$
0.01	150/155	57.7%	52.5%	0.15114	27.81	64.02
1.0	56/61	56.5%	51.5%	0.12165	28.13	63.90
10	23/15	54.1%	46.0%	0.15559	30.06	65.75

Table 2: Same as experiment in Tab. 1, but run on the CIFAR100 dataset. **Top:** Resnet-32. **Bottom:** SimpleCNN.

γ	$ \mathbf{H} _F$	Test acc.	Val. acc. (50)	Loss	Dist.	$\rho(W)$
0.01	94/185	90.2%	86.9%	0.09854	36.10	231.06
1.0	20/28	90.0%	84.9%	0.10232	35.95	228.01
5	0/0	89.6%	82.0%	0.11102	35.12	217.69

γ	$ \mathbf{H} _F$	Test acc.	Val. acc. (50)	Loss	Dist.	$\rho(W)$
0.01	36/51	88.7%	86.8%	0.00016	60.38	118.42
1.0	1/1	88.4%	86.3%	0.00011	60.77	118.71
5	0/0	88.5%	85.6%	0.00098	63.12	120.86

Table 3: Same as experiment in Tab. 1, but run using momentum (0.9). **Top:** Resnet-32. **Bottom:** SimpleCNN.

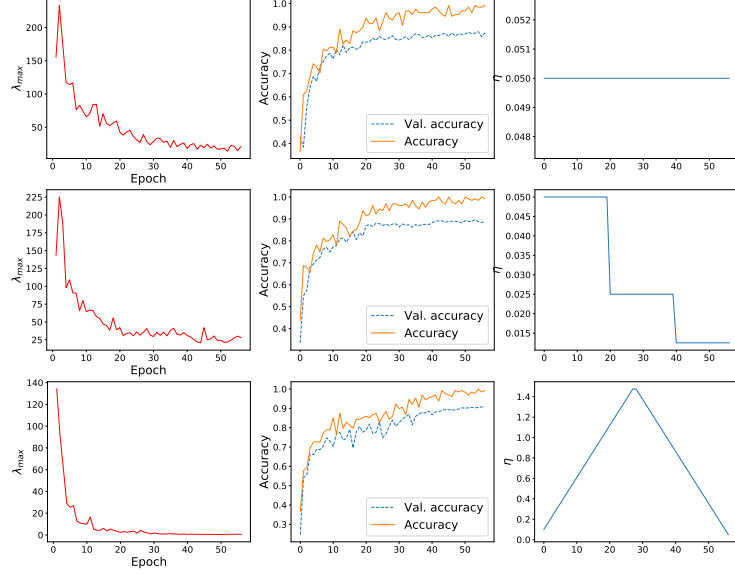


Figure 15: Evolution of $\rho(\mathbf{H})$ (first column), accuracy (middle) for different learning rate schedules (learning rate used in each epoch is plotted in the last column). Top is constant η , middle is step-wise decaying η and bottom is a single cycle learning rate schedule. Note different scale on the y axes between the plots.

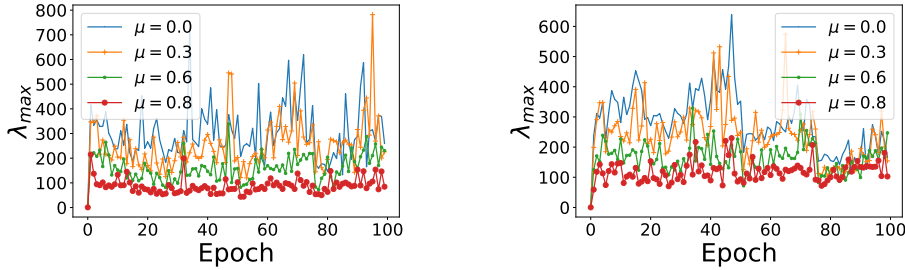


Figure 16: Momentum reduces spectral norm of the Hessian. Training at $\eta = 0.1$ and $S = 128$ on VGG11 and CIFAR10 (left) and CIFAR100 (right).

F SimpleCNN Model

The SimpleCNN used in this paper has four convolutional layers. The first two have 32 filters, while the third and fourth have 64 filters. In all convolutional layers, the convolutional kernel window size used is (3,3) and ‘same’ padding is used. Each convolutional layer is followed by a ReLU activation function. Max-pooling is used after the second and fourth convolutional layer, with a pool-size of (2,2). After the convolutional layers there are two linear layers with output size 128 and 10 respectively. After the first linear layer ReLU activation is used. After the final linear layer a softmax is applied.